Manuscript title:

A comparison of bacterial communities from OMZ sediments in the Arabian Sea and the Bay of Bengal reveals major differences in nitrogen turnover and carbon recycling potential

Author names:

[1, 2]Jovitha Lincy [*] and [1]Cathrine Sumathi Manohar

Author affiliation(s):

[1] Biological Oceanography Division, CSIR-National Institute of Oceanography (NIO), Goa-403004, India.

[2] Academy of Scientific and Innovative Research (AcSIR), CSIR-NIO Campus, Goa, India.

Correspondence:

JL: jovithalincy@gmail.com**; +91-9847871900** ([*]corresponding author)**.**

CSM: cathrine@nio.org**; +91-832-245-0441.**

ABSTRACT:

The Northern Indian Ocean hosts two Oxygen Minimum Zones (OMZ), one in the Arabian Sea and the other in the Bay of Bengal. High-throughput sequencing was used to understand the total bacterial diversity in, the surface sediment off Goa within the OMZ of the Arabian Sea, and from off Paradip within the OMZ of the Bay of Bengal. The dominant phyla identified included Firmicutes (33.08%) and Proteobacteria (32.59%) from the Arabian Sea, and Proteobacteria (52.65%) and Planctomycetes (9.36%) from the Bay of Bengal. Only 30% of OTUs were shared between the sites which make up three-fourth of the Bay of Bengal OMZ bacterial community, but only one-fourth of the Arabian Sea OMZ sediment bacterial community. Statistical analysis indicated the bacterial diversity from sediments of the Bay of Bengal OMZ is ~48% higher than the Arabian Sea OMZ. The community analysis combined with a predictive functional profiling of 16S rRNA amplicons pinpointed the occurrence of specific enzymes that are crucial in the cycling of nitrogen and sulfur compounds, with major differences regarding nitrogen fixation and carbon recycling.

Keywords:

OMZ, sediment bacteria, 454 pyrosequencing, Arabian Sea, Bay of Bengal, functional ecology.

1. INTRODUCTION

The Northern Indian Ocean consists of two major ocean basins: the Arabian Sea (AS) in the west and the Bay of Bengal (BoB) in the east. Even though both these basins are placed in the same latitude, they differ in many aspects. This includes differences in average salinity, primary productivity, nitrogen loss, the intensity of mesoscale eddies, contrasting transport of dissolved oxygen~~,~~ and organic matter (McCreary Jr et al., 2013). Both these basins experience intense oxygen depletion below the mixed layer of the water column, where dissolved oxygen (DO) is usually below the detection limit of conventional methods. The AS-OMZ between the water depths of ~100/150 – 1000/1200m is the thickest OMZ, and is identified as a primary site of fixed nitrogen loss (Naqvi et al., 2006). In contrast, ~~in~~ the BoB-OMZ has been reported less intense than the AS-OMZ (Paulmier, 2009) with DO concentrations still present in the nanomolar range (Bristow et al., 2017). Nitrogen loss has been described as rather insignificant and limited by substrate availability resulting from low organic matter supply by primary production (Bristow et al., 2017;Löscher et al., 2020). The sequence of electron acceptor utilization in such an environment, generally follow the thermodynamic energy yield (Froelich et al., 1979). However,

recent studies support the possibility of co-occurrence of metabolisms using different electron acceptors in OMZs, one example would be the existence of a cryptic sulfur cycle, which occurs along with nitrogen cycle processes (Callbeck et al., 2018;Canfield et al., 2010).

Surface sediment underlying OMZs entraps all recent microbial signatures of the water column above (Gerdes et al., 2000) in addition to the sediment microbiome; hence it is interesting to explore and compare such benthic OMZ ecosystems, especially those located in shallow zones. OMZs act as niches for microorganisms that can use alternative pathways of respiration (Diaz and Rosenberg, 2008;Pitcher et al., 2011). In the BoB-OMZ, aerobic communities have identified to coexist with anaerobic communities (Bristow et al., 2017). In the AS, such coexistence was explained by separate micro-niches in the same environment (Pitcher et al., 2011). Similar studies carried out in eastern AS-OMZ sediments have identified Proteobacteria (52%) and Planctomycetes (12.7%) as the dominant phyla (Divya et al., 2011). Other integral phyla of soil/sediment habitat are Bacteroidetes, Acidobacteria, Actinobacteria, and Firmicutes (Lv et al., 2014).

It is vital to understand the dominant microbial taxa and also their functional ecology to throw light on the biogeochemistry of these oxygen-depleted zones (Rajpathak et al., 2018). With the advent of molecular techniques over the last decade, a large volume of data has been generated which helped to elucidate the bacterial community structure (Hodkinson and Grice, 2015). Phylogenetic profiling, using next-generation sequencing (NGS) techniques, offer high-resolution data from complex environments (Claesson et al., 2010). By using algorithms leveraging functional databases, it is also possible to predict putative functional ecology from 16S rRNA amplicon data. The available data on the bacterial community structure of the northern Indian Ocean OMZ using such high-throughput sequencing techniques has ~~chiefly~~ been limited to the pelagic realm (Fernandes et al., 2019;Rajpathak et al., 2018), or restricted to some functionally significant groups rather than total bacterial community (Fernandes et al., 2018). Descriptions of OMZ sediment bacterial communities are largely underrepresented and need special attention.

The objective of our work was to compare the surface sediment bacterial diversity within two major OMZs in the northern Indian Ocean, the Arabian Sea (AS) and the Bay of Bengal (BoB), using NGS on the v1-v3 hypervariable region of the 16S rRNA gene. Based on this high throughput sequencing dataset, we predicted the metabolic potential present at both sites, the AS and the BoB with a key focus on genes relevant for nitrogen and sulfur turnover.

2. MATERIALS & METHODS

2.1. Sample collection and site characteristics

Sediment samples were collected in February 2013 off Goa in the AS-OMZ (SSK-046, *RV Sindhu Sankalp*), at the GS1A site located at $15^0$13'N, $72^0$56'E, and in August 2014 off Paradip in the BoB (SSD-002, *RV Sindhu Sadhana*)., at the PS1B site located at $19^0$57'N, $86^0$46'E (Fig.1-A). A ~~typical~~ ~~OMZ~~ profile is ~~added~~ from the AS and BoB, respectively. ~~Those~~ profiles represent typical conditions for the two sampling locations but were obtained from other cruises and show the distribution of dissolved oxygen, nitrate and nitrite from the surface to 1000m water depth in μM (Fig.1-B-C). Sampling at both stations covered surface sediments below a ~200m deep water column, underlying OMZ waters. Though both areas experience intense oxygen depletion with the core of the OMZ located between 150 and 500 m, the maximum NO_x values are twice as high in the AS as compared to the BoB, with a prominent secondary nitrite maxima (SNM). A box corer was used to retrieve the sediment samples. The sediment cores were carefully sub-sampled using acrylic core liners (25 mm ID, ~30 cm length), sub-samples were taken from the center of the core to avoid mixing of sediment layers. The 0-5 cm subsections of samples were transferred into sterile screw-cap containers. Samples were handled sterile and preserved at -20°C until further analysis. The Temperature/Salinity profiling of the water column above the sediment was carried out using a Sea-Bird Electronics conductivity-temperature-depth (CTD) sensor (SBE9), equipped with a Niskin bottle rosette sampling system, and a dissolved oxygen (DO) sensor (RINKO, ALEC, Japan).

2.2. Sediment characterization

The sediments were freeze-dried, homogenized, and ground in an agate mortar prior analysis. Total carbon (TC) comprising both inorganic and organic carbon, and total nitrogen (TN) comprising dissolved and particulate nitrogen and all forms of inorganic nitrogen derivatives were analyzed in an elemental carbon/ nitrogen (CN) analyzer (FISONS NA1500) using the method described in (Bhushan et al., 2001). The calibration of the CN analyzer was done using a reference standard (NC-soil), and the obtained recovery rate was 96% for TC and 99% for TN. The precision was monitored by carrying out replicates for both samples and was ±1%. The detection limits were two times the blank value. Total organic carbon (TOC) contents were determined with a colorimetric based wet oxidation method (Azam and Sajjad, 2005), which is reported to be highly reproducible. Inorganic carbon (TIC) was determined as the difference between TC and TOC (Bernard et

al., 1995). Organic matter (OM) was calculated by multiplying TOC with the Van Bemmelen's factor 1.724 (Heaton et al., 2016), based on the assumption that humidified organic matter of soil contains 58% carbon, however, variations of 40-60% have been observed (Nelson and Sommers, 1982). For determining $CaCO_3$ abundances, TIC was multiplied with a factor of 8.33 to get the percent calcium carbonate as described previously (Bernard et al., 1995).

2.3. Genomic DNA extraction and 454 Pyrosequencing

Total genomic DNA was extracted from 400-500 mg of the sediment samples in triplicates, using the Fast DNA™ SPIN Kit for Soil (MP Biomedicals, Santa Ana, CA). The purified DNA was quantified using a Nanodrop 2000 spectrophotometer (ThermoScientific, USA). DNA was quality checked on an agarose gel (0.8%). The extracted DNA was pooled and amplified using barcoded fusion primers targeting the v1–v3 region of the 16S rRNA gene using the universal primer 9F (AGAGTTTGATCMTGGCTCAG) and 541R (ATTACCGCGGCTGCTGG). Mixed amplicons were subjected to emulsion PCR and then deposited on picotiter plates (Agilent, USA). Amplification conditions consisted of an initial denaturation step at 95°C for 5 min, followed by 30 cycles of denaturation at 95°C for 30 sec, annealing at 55°C for 30 sec, and elongation at 72°C for 30 sec, with a final elongation at 72°C for 5 min. The detailed procedure of pyrosequencing is described elsewhere (Suh et al., 2014). Sequencing was performed by Chunlab Inc. (Seoul, Korea) using a 454 GS FLX Titanium Sequencing system (Roche Branford, CT, USA) per the manufacturer's instructions.

2.4. Sequence data processing

Amplicon pyrosequencing data were processed using the QIIME software package, ver. 1.7. (Caporaso et al., 2010). Chimaeras and primer mismatch sequences were removed from the amplicon dataset using the Amplicon Noise software, version 1.27 (Quince et al., 2011) available from the FLX Titanium sequence data platform, and implemented in QIIMEa using the program CD-HIT (Edgar, 2010). The average read length of PCR amplicons was 378±45 bp. The resulting reads were taxonomically classified based on similarity scores in both the basic local search tool (BLASTN) searches (E-value $>10^{-5}$) on the EzTaxon-e 16S rDNA database (2014.07.01) and on the SILVA SSU database, release 132, based on the RDP classifier method (version14) (Im et al., 2012). Relative abundances of taxonomic groups were estimated using the following cut-off values: species ($x \geq 97\%$), genus ($97\% > x \geq 94\%$), family ($94\% > x \geq 90\%$), order ($90\% > x \geq 85\%$), class ($85\% > x \geq 80\%$) and phylum ($80 > x \geq 75\%$). If the similarity was lower than the specific cut-off value, the sequence was

characterized unclassified (un) (Chun et al., 2007); sequences ~~which~~ didn't have any cultivable representatives were shortened as 'ucl.' The diversity indices and rarefaction curves were calculated at 97% sequence similarity using the Mothur platform v.1.43.0. (Schloss et al., 2009). The CLCommunity™ software version 3.46 was used for data visualization. Venn diagrams were used to compare sediment bacterial taxonomic composition between sampling sites.

Out of 17,784 reads, 43% were filtered out during the quality processing. After read pre-processing, 5944 reads for the AS sediment, and 4125 reads for the BoB sediment sample were available for further analysis with a mean length of approx. 470-480 bp. In marine sediments, pyrosequencing read numbers varied between 5,000 and 20,000 per sample in previous studies (Zhu et al., 2013;Choi et al., 2016), the output of our sequencing approach is in the same order of magnitude. The taxonomic assignment done using the SILVA platform (Quast et al., 2012) resulted in classifying the bacterial sequences into several specific clades, the EzTaxon-e data analysis (Chun et al., 2007) was used for species-level taxonomic assignment.

2.5. Functional prediction of 16S rRNA amplicons

For the functional prediction of 16S rRNA pyrosequencing amplicons, the OTUs were clustered at 97% sequence similarity. The OTU table and representative sequence fasta files were submitted to the Piphillin pipeline (https://piphillin.secondgenome.com/) (Iwai et al., 2016). The Piphillin algorithm has the advantage to not rely on phylogenetic trees to predict metagenomic contents. It further uses more recent releases of the functional database Kyoto Encyclopedia of Genes and Genomes (KEGG, updated Oct 2018)) and BioCyc ~~as~~ compared to alternative pipelines such as PICRUSt or Tax4Fun (Narayan et al., 2020). It utilizes nearest-neighbor matching 16S rRNA amplicons (or genomes) to predict the representative genomes. The normalized 16S rRNA copy number of each genome is inferred using gene content collected in functional databases (Langille et al., 2013;Iwai et al., 2016;Narayan et al., 2020).The KEGG reference database was used at a 90% cutoff level to predict metabolic functions present in the sequenced microbial community. The final output of this workflow was quantified in terms of predicted gene abundances per number of OTUs per sample. The information extracted was based a small fraction of the population available from the KEGG database. At 90% similarity cut off, around 338 KEGG pathways were identified from 156 OTU representatives from the AS and 354 KEGG pathways for 469 OTUs from the BoB. We focused on the KEGG database pathways for nitrogen (ko00910), sulfur (ko00920), and methane (ko00680) turnover, as well as on carbon metabolism (ko01200) with specific focus on fermentation and bioenergetics pathway related to carbon fixation.

3. RESULTS AND DISCUSSION

3.1. Sediment biogeochemistry

In the present study, both sampling sites showed intense oxygen depletion with dissolved oxygen (O_2) concentrations of 2±0.4 µM. In the shallow zones of BoB-OMZ and in the AS, the DO concentration sometimes falls below the detection limit of conventional methods, especially during the summer monsoon, due to the increased riverine nutrient loading, coastal high primary production and increased respiration (Sarma et al., 2013). Between both sampling sites, bottom water salinity was comparable, but the temperature differed by 3°C, which may be a seasonal or permanent feature. The sample characteristics of the collected sediment and near-bottom waters are presented in Table 1. In brief, total organic carbon was slightly higher in the AS with 3.47% and 2.24% ~~in the BoB~~, TN values were 0.28% and 0.16% in the AS and BoB, respectively. The TOC/TN ratio was 8.28 in the AS, and 7.174 in the BoB, thus conditions in the organic matter pool were rather comparable. The only striking difference was observed regarding TOC and TN values are in the typical range of OMZ sediments and higher than non-OMZ surface sediments with TOC and TN values as low as 0.2 and 0.02 wt. % (Pattan et al., 2013). OMZs enhance the preservation of organic matter, explaining the reported values of TOC ranging from ~1-2 to 6-7% (Cowie et al., 2014) and TOC/TN ratios within 7.3 – 12.3 (van der Weijden et al., 1999). Our data is in line with those OMZ-~~typical~~ ranges, with somewhat lower concentrations for both, TOC and TN, in sediments of the BoB. This may result from generally assumed lower productivity of BoB waters compared to the AS rapid nitrogen burial as described for OMZ sediments (Robinson et al., 2012), or different activities in re-mineralization processes (Bohlen et al., 2011). TIC, which was substantially higher in the AS ~~with~~ 8.11%, compared to the BoB with only 0.29%.

While in the range of OMZ sediments and higher than the difference in TIC could be attributed to the difference in $CaCO_3$ content caused by increased carbon sequestration (Sarma et al., 2007). Additionally, ~~shelled~~ meiobenthic fauna may contribute to the difference in TIC, as this is found to be abundant in sediments of the AS while not abundant in the BoB (Ramaswamy and Gaye, 2006). Besides, different microbial communities could explain patterns of carbonate precipitation, a possibility which we will explore in the following.

3.2. Bacterial diversity in Indian Ocean sediments

Between the studied sites, the BoB sediments harbor a more diverse bacterial community than the sediments of the AS, which is illustrated not only by the general diversity of taxa and in line with the few available other studies (Fig. 3) (Zhu et al., 2013;Dang et al., 2008)) but also corroborated by various diversity measures as presented in Table 2. Given that our rarefaction analysis (A1) showed that our sequencing approach was able to recover ~70% of bacterial phylotypes from the BoB and 90 % from the AS sediments, the diversity in the BoB is however still rather underestimated and may be even higher.

The dominant communities and their relative percentage remained the same for BLASTN searches using the EzTaxon-e 16S database, where a total of 48 phyla were identified, and pairwise alignment using the SILVA 132 database. This led to a successful in classification of 44 phyla, 27 of which were common to both sites. Generally, the dominant bacterial phyla consisted of Firmicutes (33.08%), Proteobacteria (32.59%), Bacteroidetes (17.48%), and Chloroflexi (5.52%) in AS sediments and Proteobacteria (52.65%), Planctomycetes (9.36%), Actinobacteria (7.25%), Firmicutes (5.5%), Acidobacteria (6.74%) and Chloroflexi (4.49%) in BoB sediments. Those abundant taxa contributed with >85% to the total bacterial community.

The dominance of Proteobacteria is well documented in marine ecosystems (Wang et al., 2012). In the eastern AS-OMZ surface sediment, nearly 14 phyla were identified in a previous study using the Sanger sequencing technique, the majority of which were Proteobacteria (52%), followed by Planctomycetes (12.7%) and Chloroflexi (8.8%) (Divya et al., 2011). Similarly, in another study carried out utilizing high-throughput sequencing confirms Proteobacteria to be the dominant phylum making up 70-75% in all six sites within benthic OMZ of AS followed by Bacteroidetes. Representative sequences affiliated to phyla Chloroflexi and Firmicutes were also recovered in a considerable number (Fernandes et al., 2018). From sediments collected from off Paradip port, which is roughly 27 nautical miles from our BoB sampling site PS1B, close to 40 bacterial phyla were reported using high-throughput methods similar to our study. The relative contribution of the phylum Proteobacteria was only 17%, which was lesser than Bacteroidetes (23%) and Firmicutes (19%) (Pramanik et al., 2016) indicating a certain patchiness in relative abundance but an overall comparability of the bacterial community composition in the BoB possibly resulting from factors including DO (Stewart et al., 2012), the availability of nutrients or organic carbon determine (Fierer and Jackson, 2006).

The candidate phyla GN02, OD1, TM6, TM7, and WS3, were prevalent in ESP (eastern south pacific) pelagic OMZ microbiome as well, implying that they have an essential role in OMZ nutrient cycling (Ulloa et al., 2013;Ganesh et al., 2014). Candidate phyla GN02, OP3, OP8, were unique to both sampled OMZs

sediments of the northern Indian Ocean. A total of 13 candidate phyla were obtained in our study. The prevalence of such "bacterial dark matter" highlights the need to decipher their coding potential, as they can't be subjected to functional predictions due to a lack of cultivable representatives.

A complete list of taxa is presented in the Supplementary information A2. Interestingly, only 28.48% of the identified OTUs were shared between the AS and the BoB on the genus level were between (64.29% on the phylum level), leaving 53.10% of unique OTUs in the BoB and 18.42% in the AS (Fig. 2). This suggests that the two sediments, while biogeochemically similar, harbor a largely different bacterial community.

The analysis of 58 bacterial classes recovered from our data set showed that there >50% similarities between the phylotypes at the two site which makes up ~97% of bacteria. The dominant classes in the AS sediment include Bacilli (32.96%), Gammaproteobacteria (18.34%) and Bacteroidia (17.19%). In the BoB sediment, Gamma-, Alpha, and Delta-Proteobacteria (23.68%, 19.01%, 9.26% respectively) were most abundant, followed by Planctomycetacia (6.72%). Those clades together contribute between 60-70% of the total in the BoB sediment. Dominant bacterial orders recovered exclusively from the AS-OMZ include Bacillales (32.94%), majorly Planococcaceae (26.06%). Flavobacteriales (17.14%), and Oceanospirillales (12.85%). In BoB sediments, Steroidobacterales (7.05%) and Rhizobiales (11.03%) form the most dominant groups. Exploring the taxonomy in more detail, relative abundances for fermenting organisms such as Planococcaceae, Flavobacteriaceae, Bacillaceae, Oceanospirillaceae, Rhodobacteraceae, and Vibrionaceae are strikingly higher in the AS sediment compared to the BoB amongst the abundant clusters (abundant >1%; Fig. 3). Those clades are mainly described as heterotroph degraders, mostly able to ferment (Glöckner et al., 1999;Yakimov et al., 2003). The presence of Alcanivoraceae in the AS sediment, and their absence in the sediment of the BoB, could be an important factor in the precipitation of $CaCO_3$, because of their metabolic capability to use ammonification and carbonic anhydrase activity to induce rapid calcium carbonate precipitation (Krause et al., 2018). In the BoB, abundant clades consist mostly of Pseudomonadaceae firstly described in a deep sea sediment from a Japanese trench [clone AB013829, (Yanagibayashi et al., 1999)] and Desulfobacteraceae, both of which are described denitrifier groups. Desulfobacteraceae often use acetate (Dyksma et al., 2018) but are also know to degrade other organic compounds (Kümmel et al., 2015). Besides those clades, different proteobacterial clades were found, as well as the purple non-sulfur bacteria Rhodobacteraceae and Rhodospirilliaceae, the latter of which are able to fix molecular nitrogen (Madigan et al., 1984). The double pie-chart provides an overview of both sequenced bacterial communities at the class and family level (Fig. 3).

In AS sediments, the most abundant bacterial genus was *Paenisporosarcina* sp. (24.06%), followed by *Salegentibacter* sp. (17%), and as per EzTaxon-e database those were ~~closer~~ identified as *Paenisporosarcina quisquiliarum* and *Salegentibacter mishustinae*. Those groups were followed by *Amphritea* (9.02%), *Oceanibulbus* (4.27%), Alcanivorax (3.82%), *Photobacterium* (2.76%) and *Salipaludibacillus* (2.61%). All of those clades ~~were~~ unique to AS sediment and not present in the BoB sediments. In BoB sediments, the most abundant taxa ~~were~~ Woeseia (6.98%) and Gammaproteobacteria_ucl (6.5%), with the remaining groups being represented with less than 3%.

The clade Woeseiaceae/JTB255 is recognized as the most abundant clade in marine sediment, having a cosmopolitan distribution. Moreover, analyzed metagenomes of JTB255 are known to encode the truncated denitrification pathway to nitrous oxide (Mußmann et al., 2017). Since denitrification mediated nitrogen loss is reported to be dominant in Arabian Sea OMZ, we expected to get more hits in the analyzed amplicon dataset (Ward et al., 2009). Though their occurrence was not detected, few representative sequences of JTB31 and JTB38 ~~have~~ identified ~~which~~ might ~~have~~ a similar role.

3.3. Predicted functional ecology

For a large proportion of the amplicons, functions could not be assigned clearly, which leads to a rather conservative, and qualitative instead of quantitative estimate of the metabolic potential present at the two sites. The predictive functional profiling of 16S rRNA sequences has identified a high proportion of genes involved in methane cycling, as generally typical for sediments underlying OMZ waters (Bertics et al., 2013;Fulweiler et al., 2007;Gier et al., 2016), followed by genes involved in sulfur and nitrogen cycling. (Fig. 4). Methane turnover rates are rather high in anoxic shelf sediments and ~~are~~ were reported to be correlated with the availability of labile organic matter, and concurrent with sulfate reduction (Maltby et al., 2016), explaining the predicted abundance of genes involved in methane turnover in our samples. Despite the difference in diversity between the two sampling sites, almost all predicted gene functions were identical suggesting an overall similar metabolic potential in the two different sediments.

Nitrogen cycle: In northern Indian Ocean OMZs, nitrogen cycling is reported to be very active (Naqvi et al., 2006). At both our sampling sites, genes coding for major nitrogen cycle pathways including nitrogen fixation, dissimilatory nitrate reduction to ammonia (DNRA), nitrification, and denitrification were predicted. Interestingly, anammox genes were not predicted for either site despite the presence of planctomycetes in our dataset (Fig.7). This may be either due to the low number of species-level identifiable OTUs or to a true absence

of anammox-capable planctomycetes as consistent with OMZ sediments from the seasonally anoxic Eckernförde Bay in the Baltic Sea and sediments underlying the Peruvian OMZ (Dale et al., 2011;Bertics et al., 2013). While generally planctomycetes were in the sequence pool, hits corresponding to anammox planctomycetes were indeed very low at our sampling sites, accounting for 0.03 and 0.3% in the AS and BoB, respectively. A sequencing related bias could, however, have led to an underestimation of *Scalindua*-anammox bacteria as a systematic underrepresentation by sequencing of 16SrDNA v1-v3 regions has been reported (Penton et al., 2006). Specifically, the functional marker gene coding for the hydrazine oxidoreductase was not predicted from our 16S rDNA data. This suggests that the contribution of anammox to the nitrogen cycle in the Indian Ocean sediments, at least at our sampling sites, is rather low similar to the pelagic OMZ of the AS where denitrification is reported to be dominant over anammox (Ward et al., 2009), and the BoB where anammox as well as denitrification could not be detected (Bristow et al., 2017) ~~active~~. As Planctomycetales are known to encode a large number of sulfatase genes, which makes them as a specialist for the initial breakdown of sulfated hetero-polysaccharides (Wegner et al., 2013), their role in the Indian Ocean sediments could rather be carbon capture in the sediments (Jensen et al., 2011;Arango et al., 2007;Shao et al., 2010;Dale et al., 2011). Here, the predicted gene abundance was 848 and 2901 for AS and BoB microbiome for the predominant form being arylsulfatase, respectively, contributing 65-85% of the sulfatase pool.

The global annual denitrification rate in sediment would be approximately 200 Tg N, and the majority contributed from sediments underlying OMZ, where its reported two to four times higher (Devol, 2015). Therefore, nitrogen loss processes would be expected to take place in both, sediments of the AS and the BoB. Denitrification and sulfite reductase genes were prevalent in our prediction possibly favoring sulfur driven autotrophic denitrification (Shao et al., 2010), and as previous studies suggested heterotrophic denitrification (Arango et al., 2007). Other denitrifiers recovered from our sequence dataset are Oceanospirillales, Chromatiales, Nitrospirales, Syntrophobacteriales, and NB1-j which are known to encode denitrification genes including *nirS, norB* and *nosZ* (de Voogd et al., 2015), and contributed 14.05% in the AS sediment, and 4.46% in the BoB sediment, respectively. Similarly, Flavobacteriales are known denitrifiers (Horn et al., 2005), and ~~was~~ are abundant in the AS with 17.14% of all 16S rDNA sequences.

Recent studies have also linked methane oxidation to nitrite-based denitrification in the Candidatus phylum NC10 (Padilla et al., 2016). This was supported by studies carried out in a freshwater reservoir, where methane stimulated massive nitrogen loss (Naqvi et al., 2018). As denitrification is reported to be dominated over anammox in the northern Indian Ocean OMZ (Ward et al., 2009), and our data confirm the same for Indian

Ocean sediments, the coupling of methane oxidation and denitrification might be a possible nitrogen loss pathway. Identified, Steroidobacter clades, which are known to perform denitrification coupled with methane oxidation (Liu et al., 2014), make up 7% of the BoB-OMZ bacterial community.

DNRA was predicted as a potential pathway in both basins of our study. In seasonally hypoxic Baltic Sea sediments, DNRA accounted for almost 75% of benthic nitrogen flux (Dale et al., 2011). In contrast to the other nitrogen cycle genes, the *nifHDK* operon coding for the functional unit of the key gene for nitrogen fixation, the nitrogenase, was predicted in higher abundance in the BoB compared to the AS, with BoB-nif being five times as many as AS-nif. This is consistent with the higher proportions of known sedimentary nitrogen fixers, such as Desulfobacteraceae and Rhodospirilliaceae. The presence of nitrogen fixers in sediments underlying OMZs has been documented for several regions, including the upwelling system off Mauretania, the Baltic Sea and the eastern tropical South Pacific shelfs, and nitrogen fixing microbes have been shown to be active although at low rates (Bertics et al., 2013;Gier et al., 2017;Gier et al., 2016).

Sulfur cycling: For the sulfur cycle in both, the AS and the BoB, genes for the assimilatory pathway of sulfate reduction were predicted, as well as sulfur oxidation genes of the *sox* operon (Fig.8) in line with a previous study which identified diverse sulfur reducing bacterial and archaeal OTUs in the AS (Fernandes et al., 2018). In our AS dataset, a potential player in the sulfur cycle could be *Sulfitobacter dubius*, which was represented with 4.32% of all OTUs. All known species of the genus *Sulfitobacter* were isolated from marine habitats and are known to perform sulfite oxidation (Sorokin, 1995;Long et al., 2011). *Thermodesulfovibrio* (phylum Nitrospira) accounted for ~1% of sequences at both sites are known sulfate reducers and have been identified from the eastern tropical South Pacific OMZ, before (Schunck et al., 2013). Sequences corresponding to sulfur reducers like Desulfobacterales (AS: 0.87%, BoB: 2.57%) and Syntrophobacterales (AS: 0.67%, BoB: 1.21%) were also recovered from our dataset and were shown to be abundant in sediments of the Black Sea sulfate-methane transition zone as well as in the Arabian Sea OMZ in both pelagic and benthic realms (Fernandes et al., 2018;Fuchs et al., 2005;Leloup et al., 2007).

Carbon fixation: In the BoB sediment, around 1.75% of gene families were predicted to perform photosynthesis, and major contributors would possibly be Chromatiales (07%), Rhodospirillales (0.03%), and members of phylum Cyanobacteria (1.65%). Chromatiales, a group of purple sulfur bacteria, can perform anoxygenic photosynthesis (Manske et al., 2005). Similarly, Rhodospirillalesis primarily chemoorganotroph and photoheterotroph (Luo and Moran, 2015), can also perform anoxygenic photosynthesis (Manske et al., 2005). It's interesting to note that around 68 Cyanobacterial sequences were retrieved from BoB sediment, where water

column depth was ~245m, but only one representative from the AS sediment, which was located at ~200m depth. In addition, in the AS sediment, we observed Chroococcales, which are assumed to be a low-light adapted group (West et al., 2001). The key enzymes responsible for energy metabolism are presented in Table-3. In particular, the higher predicted abundance of dehydrogenase enzymes responsible for oxidation of organic matter in the AS points towards a difference in carbon metabolism in the two regions. This is most likely due to the increased availability of carbon in the AS, however, as proposed earlier (Orsi et al., 2017), more efficient organic carbon recycling in the AS may over geological timescales contribute to developing a stronger and more persistent functional anoxia.

Carbon remineralization: As indicated by the high TIC concentration in the AS sediment, carbon remineralization was very active due to the increased availability of organic carbon (Yu et al., 2018). About 20% of the identified bacteria were common soil/sediment inhabitants with a prime role ~~is~~ remineralization of diverse organic carbon compounds (Schimel and Schaeffer, 2015). These include Acidobacteria, Actinobacteria, Bacteroidetes, and Gemmatimonadetes (Janssen, 2006). Similarly, Anaerolinaeles (phylum Chloroflexi), which contributed 2-3% of the total hits in our dataset, have also been identified with a similar role and were specific to areas that show very low or zero oxygen. In addition, genes responsible for N-glycan degradation (ko00511) were predicted to occur almost twelve times more often in the AS than in the BoB sample. These genes play a role in cell adhesion and sequestration (Varki and Gagneux, 2017). The relative distribution of key enzymes and genes specific to gram-positive and gram-negative bacterial fermenters were compared based on previous reports (Ramos et al., 2000;Eschbach et al., 2004) (Fig.6). Their predicted abundance was higher in AS sediment than in BoB sediments. The connected more complete carbon remineralization which could add an explanation to why the AS-OMZ is more anoxic than the BoB-OMZ as previously suggested (Orsi et al).

4. CONCLUSION

We compared bacterial communities from two sites in the northern Indian Ocean OMZ, in the BoB off Paradip and a site off Goa in the AS. Less than one-third of the phylotypes were shared between the two sites, leaving a large individual proportion of the bacteria for each site. A higher diversity has been identified from the BoB, compared to the AS, however, our functional prediction identified high abundances of typical heterotrophic degraders in the AS, that were only represented in low proportions or absent in the BoB. We further identified denitrifiers, DNRA bacteria and sulfur cycle bacteria at both sites and predicted the presence

of their functional genes. The higher functional diversity for organic matter degradation with fermentation in addition to denitrification and sulfur-compound dependent remineralization may explain, why the AS OMZ is generally more anoxic. Here, the variability in carbon respiration pathways may allow for a more efficient or complete respiration along the electron tower, thus consuming more oxidized compounds. The abundance of Alcanivorax-like bacteria in AS sediments may provide an explanation for high CaCO3 precipitation, as this organism has been described to perform this process rapidly when organic nitrogen is available as it is at our sampling site in the AS. A notable finding was the absence of anammox bacteria at both sites. Notably, we predicted nitrogen fixation genes from BoB sediments but not from AS sediments, possibly resulting from higher nitrogen inputs from the water column in the AS.

Despite the limitation of this study with regard to our sample number, we could contribute a first assessment of bacterial diversity and functionality in coastal sediments of the two Indian Ocean basins, as such, we hope to contribute to the general understanding of how these basins ~~wok~~ and why they are so different in their biogeochemistry.

DATA AVAILABILITY

All pyrosequencing reads were submitted to the NCBI Genebank database under accession number KU821783 - KU831324 and MG860544 - MG860851. The supporting information is available as supplementary information.

APPENDICES

A1: Rarefaction curve of bacterial OTUs (operational taxonomic units) associated with sediments underlying oxygen-depleted waters in the northern Indian Ocean OMZ.

A2: Taxonomic composition of bacterial OTUs analyzed through the SILVA database.

AUTHOR CONTRIBUTION

JL prepared the manuscript and performed the experiments and bioinformatics analysis. CSM conceived the idea and designed the experiment.

COMPETING INTERESTS

The authors declare that they have no conflict of interest.

FUNDING

The first author is grateful to the Council of Scientific and Industrial Research (CSIR), India, for fellowship grant 31/026(0245)/2012-EMR-I for doing a Ph.D. This work is supported by CSIR grant: PSC0108. NIO's contribution no: xxxx.

ACKNOWLEDGMENT

We thank the Director of CSIR-NIO for providing the facilities. We acknowledge Chun Lab, Seoul, South Korea, for carrying out pyrosequencing. Special thanks to Dr. Carolin Löscher for the critical comments and valuable suggestions which have significantly helped in improvising the content. We express our gratitude to Dr. Amal Jayakumar, Dr. N. Ramaiah and Dr. Peter Burkill for guidance in manuscript preparation. We also thank crew members of SSK-046 and SSD-002, especially Ms. Larissa Menezes, for GS1A sample collection.

LEGENDS

Table 1: Sediment and bottom water characteristics for the samples collected from the northern Indian Ocean OMZ.

Table 2: Summary of pyrosequencing results and statistical analysis of bacterial sequences retrieved from the northern Indian Ocean OMZ surface sediment samples.

*OTUs (operational taxonomic unit) were calculated using Mothur (3% distance).

§Good's coverage is proportional to non-singleton phylotypes.

Table 3: Distribution of key enzymes relevant in energy metabolism in the northern Indian Ocean surface sediments predicted from 16S rRNA genes.

Fig. 1: A) Station map, blue dots indicate sampling stations, red dots are the regions where OMZ water-column characteristics were obtained from. B) Representative water column profiles of biogeochemical parameters from (B) the AS-OMZ (Unpublished data, personal communication from Dr. G.V.M. Gupa) and C) the BoB- OMZ (Sarma et al., 2013).

Fig. 2: Venn diagram showing OTU number wise comparison of the phylotypes at different taxonomic level assigned through the SILVA database.

Fig. 3: Dominant bacterial taxa retrieved at 1% cut-off based on pairwise alignment in the SILVA SSU database release 132.

Fig. 4: Double Pie chart showing bacterial community composition at the class and family level from the sampling locations based on the EzTaxon-e database.

Fig. 5: Relative distribution of redox metabolic KEGG pathways identified from our 16S rRNA amplicon pyrosequencing dataset utilizing the Piphillin algorithm.

Fig. 6: Percentage distribution of key enzymes with coding genes identified in bacterial fermentation (Ramos et al., 2000;Eschbach et al., 2004).

Fig. 7: Proposed pathway for OMZ Nitrogen cycling in sediments of northern Indian Ocean OMZ, and the abundance of enzymes with coding genes are indicated in box, where 'blue' and 'red' denotes AS and BoB gene count. Expansion of abbreviation are as follows:- **amoA:** Ammonia monooxygenase subunit A; **gdh:** Glutamate dehydrogenase; **hao:** Hydroxylamine oxidoreductase; **hzo:** Hydrazine oxidoreductase; **hzs:** Hydrazine synthase; **napA:** Nitrate reductase (cytochrome); **nasA:** Nitrate reductase; **narG:** Nitrate reductase, alpha subunit; **nifH:**

462 Nitrogenase iron protein; **nirK/nirS:** Nitrite reductase subunit K/S; **norB/norC:** Nitric oxide reductase subunit
463 B/C; **nrfA:** nitrite reductase (cytochrome c-552); **nosZ:** Nitrous oxide reductase; **nxrA:** nitrite oxidoreductase,
464 alpha subunit; **ureC:** Urease subunit alpha.
465 **Fig. 8:** Proposed pathway for OMZ Sulfur cycling in sediments of northern Indian Ocean OMZ, and the
466 abundance of enzymes with coding genes are indicated in box, where 'blue' and 'red' denotes AS and BoB gene
467 count. Expansion of abbreviation are as follows:- **aprA:** Adenylylsulfate reductase, subunit A; **dsrA/dsrB:**
468 Dissimilatory sulfite reductase subunit-alpha/beta; **dsrC:** Dissimilatory sulfite reductase related protein; **cysC:**
469 Adenylylsulfate kinase; **cysH:** Phosphoadenosine phosphosulfate reductase; **psrA:** Thiosulfite reductase; **rDsr:**
470 Reverse dissimilatory sulfite reductase; **sat:** Sulfate adenylyltransferase; **soeA:** Sulfite:quinone oxidoreductase;
471 **sir:** Sulfite reductase (ferredoxin); **soxB:** S-sulfosulfanyl-L-cysteine sulfohydrolase; **soxC:** Sulfane
472 dehydrogenase; **soxD:** S-disulfanyl-L-cysteine oxidoreductase; **soxX/A:** L-cysteine S-thiosulfotransferase;
473 **soxY/Z:** Sulfur-oxidizing protein; **sseA:** Thiosulfate/3-mercaptopyruvate sulfurtransferase; **sqr:** Sulfide:quinone
474 oxidoreductase; .
475
476
477
478
479
480
481
482
483
484
485
486
487

TABLES

Table 1

Sampling Details			Sediment Characteristics						Near-bottom water profile (CTD)		
Station code	Date	Sampling depth	TOC	TIC	TN	CaCO3	OM	TOC/TN	DO	Temp	Salinity
			%						μM	°C	PSU
GS1A	Feb-2013	200m	2.012	8.11	0.28	67.556	3.469	7.174	2.313	15.584	35.345
PS1B	Aug-2014	244m	1.297	0.289	0.157	2.407	2.236	8.279	1.666	12.326	35.018

Table 2

Sample name	Optimized reads	OTU richness*				OTU diversity*		Good's coverage§
		Observed	Chao1	ACE	Jackknife	Shannon	Simpson	
GS1A	5,944	955	2,506	4,305	3,450	4.37	0.934	0.893
PS1B	4,125	1,889	4,447	7,616	6,242	6.97	0.998	0.695

Table 3

ENERGY METABOLISM	KEGG	ENZYMES	GS1A	PS1B
Kreb cycle, NADH+H^+	K00161	pyruvate dehydrogenase E1 component alpha subunit [EC:1.2.4.1]	836	454
Kreb cycle, NADH+H^+	K00627	pyruvate dehydrogenase E2 component (dihydrolipoamide acetyltransferase) [EC:2.3.1.12]	1279	1108
Kreb cycle, NADH+H^+	K00382	dihydrolipoamide dehydrogenase [EC:1.8.1.4]	2476	1889
Kreb cycle, NADH+H^+	K00031	isocitrate dehydrogenase [EC:1.1.1.42]	993	1345
Kreb cycle, NADH+H^+	K00164	2-oxoglutarate dehydrogenase E1 component [EC:1.2.4.2]	895	850
Kreb cycle, GTP	K01902	succinyl-CoA synthetase alpha subunit [EC:6.2.1.5]	1064	952
Kreb cycle, $FADH_2$	K00239	succinate dehydrogenase / fumarate reductase, flavoprotein subunit [EC:1.3.5.1 1.3.5.4]	902	906
Kreb cycle, NADH+H^+	K00024	malate dehydrogenase [EC:1.1.1.37]	1051	881
Glycolysis, ATP	K00927	phosphoglycerate kinase [EC:2.7.2.3]	898	953
Glycolysis, ATP	K00873	pyruvate kinase [EC:2.7.1.40]	955	1012
Glycolysis, NADH+H^+	K00134	glyceraldehyde 3-phosphate dehydrogenase [EC:1.2.1.12]	2125	1176
Glyoxylate cycle, NADH+H^+	K00024	malate dehydrogenase [EC:1.1.1.37]	1051	881
Glyoxylate cycle, $FADH_2$	K00240	succinate dehydrogenase / fumarate reductase, iron-sulfur subunit [EC:1.3.5.1 1.3.5.4]	916	926
Pentose phosphate pathway, NADPH	K00036	glucose-6-phosphate 1-dehydrogenase [EC:1.1.1.49 1.1.1.363]	678	856
Pentose phosphate pathway, NADPH	K00033	6-phosphogluconate dehydrogenase [EC:1.1.1.44 1.1.1.343]	823	807
Ethylmalonyl pathway, $NADP^+$	K14446	crotonyl-CoA carboxylase/reductase [EC:1.3.1.85]	230	276
Ethylmalonyl pathway, GTPase activity	K01847	methylmalonyl-CoA mutase [EC:5.4.99.2]	1386	669
Ethylmalonyl pathway, $NADP^+$	K00023	acetoacetyl-CoA reductase [EC:1.1.1.36]	309	345
Ethylmalonyl pathway, ADP +Pi	K01965	propionyl-CoA carboxylase alpha chain [EC:6.4.1.3]	575	329
Ethylmalonyl pathway, ADP +Pi	K01966	propionyl-CoA carboxylase beta chain [EC:6.4.1.3 2.1.3.15]	746	351
Malonate semialdehyde pathway, ADP+Pi	K01961	acetyl-CoA carboxylase, biotin carboxylase subunit [EC:6.4.1.2 6.3.4.14]	1212	938
Propanoyl-CoA metabolism, ADP+Pi	K01965	propionyl-CoA carboxylase alpha chain [EC:6.4.1.3]	575	329

FIGURES

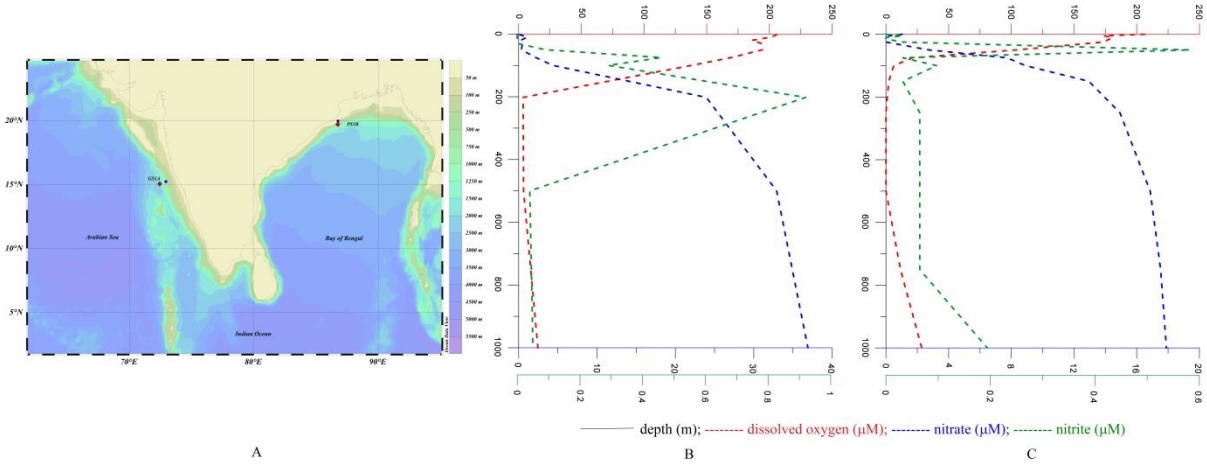

Fig. 1

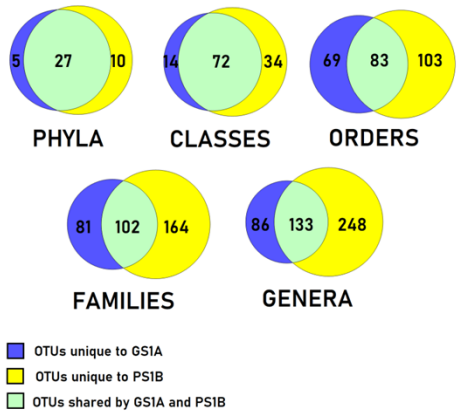

Fig. 2

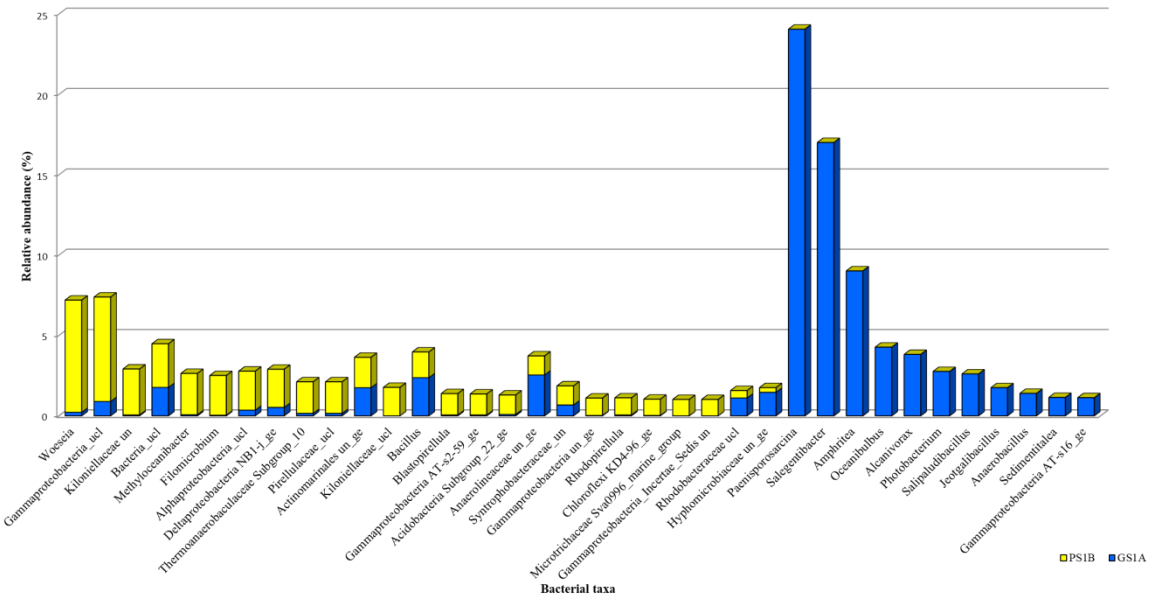

Fig. 3

Fig. 3

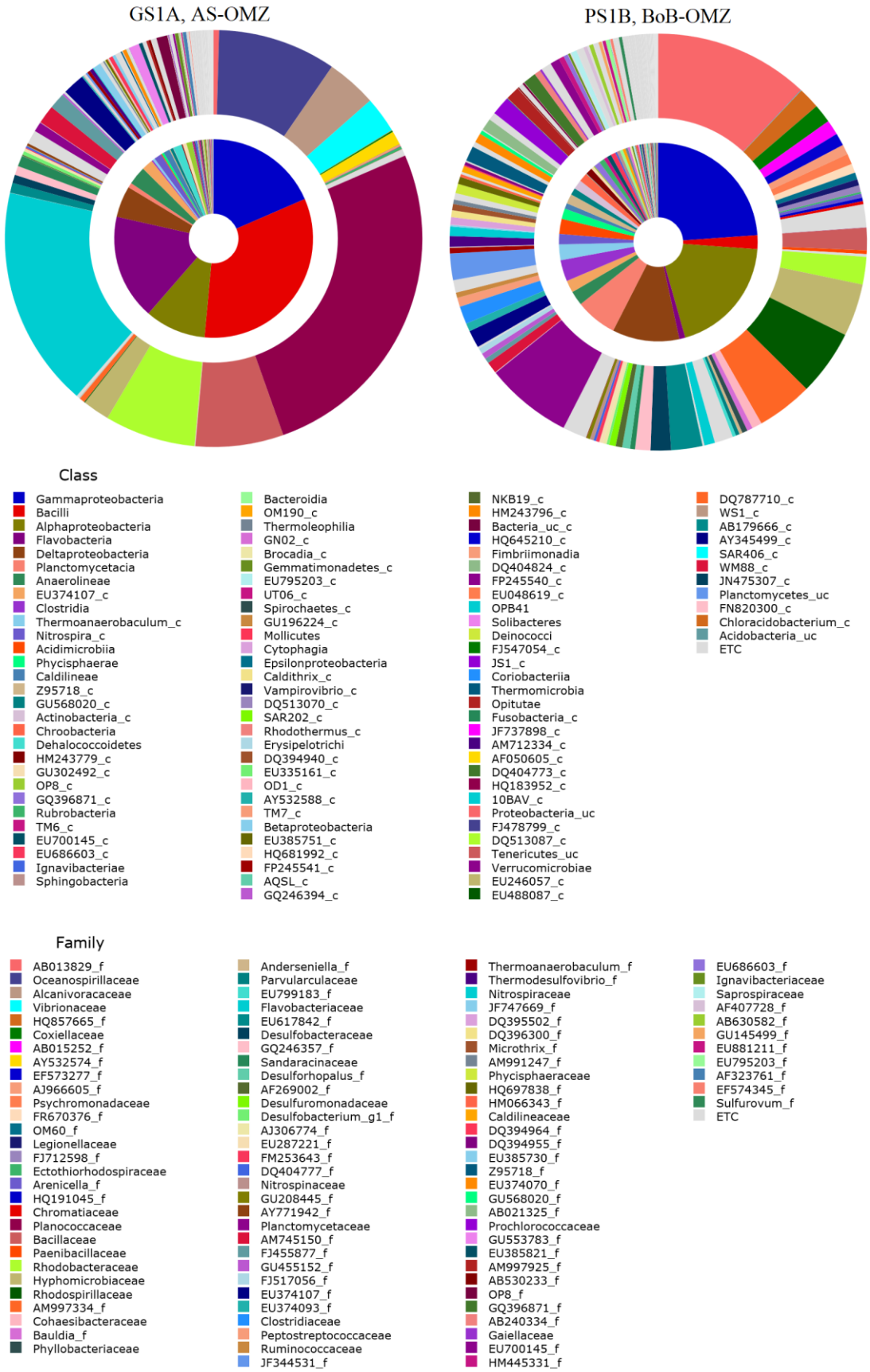
GS1A, AS-OMZ
PS1B, BoB-OMZ
Class
Gammaproteobacteria
Bacilli
Alphaproteobacteria
Flavobacteria
Deltaproteobacteria
Planctomycetacia
Anaerolineae
EU374107_c
Clostridia
Thermoanaerobaculum_c
Nitrospira_c
Acidimicrobiia
Phycisphaerae
Caldilineae
Z95718_c
GU568020_c
Actinobacteria_c
Chroobacteria
Dehalococcoidetes
HM243779_c
GU302492_c
OP8_c
GQ396871_c
Rubrobacteria
TM6_c
EU700145_c
EU686603_c
Ignavibacteriae
Sphingobacteria
Bacteroidia
OM190_c
Thermoleophilia
GN02_c
Brocadia_c
Gemmatimonadetes_c
EU795203_c
UT06_c
Spirochaetes_c
GU196224_c
Mollicutes
Cytophagia
Epsilonproteobacteria
Calditrix_c
Vampirovibrio_c
DQ513070_c
SAR202_c
Rhodothermus_c
Erysipelotrichi
DQ394940_c
EU335161_c
OD1_c
AY532588_c
TM7_c
Betaproteobacteria
EU385751_c
HQ681992_c
FP245541_c
AQSL_c
GQ246394_c
NKB19_c
HM243796_c
Bacteria_uc_c
HQ645210_c
Fimbriimonadia
DQ404824_c
FP245540_c
EU048619_c
OPB41
Solibacteres
Deinococci
FJ547054_c
JS1_c
Coriobacteriia
Thermomicrobia
Opitutae
Fusobacteria_c
JF737898_c
AM712334_c
AF050605_c
DQ404773_c
HQ183952_c
10BAV_c
Proteobacteria_uc
FJ478799_c
DQ513087_c
Tenericutes_uc
Verrucomicrobiae
EU246057_c
EU488087_c
DQ787710_c
WS1_c
AB179666_c
AY345499_c
SAR406_c
WM88_c
JN475307_c
Planctomycetes_uc
FN820300_c
Chloracidobacterium_c
Acidobacteria_uc
ETC
Family
AB013829_f
Oceanospirillaceae
Alcanivoracaceae
Vibrionaceae
HQ857665_f
Coxiellaceae
AB015252_f
AY532574_f
EF573277_f
AJ966605_f
Psychromonadaceae
FR670376_f
OM60_f
Legionellaceae
FJ712598_f
Ectothiorhodospiraceae
Arenicella_f
HQ191045_f
Chromatiaceae
Planococcaceae
Bacillaceae
Paenibacillaceae
Rhodobacteraceae
Hyphomicrobiaceae
Rhodospirillaceae
AM997334_f
Cohaesibacteraceae
Bauldia_f
Phyllobacteriaceae
Anderseniella_f
Parvularculaceae
EU799183_f
Flavobacteriaceae
EU617842_f
Desulfobacteraceae
GQ246357_f
Sandaracinaceae
Desulforhopalus_f
AF269002_f
Desulfuromonadaceae
Desulfobacterium_g1_f
AJ306774_f
EU287221_f
FM253643_f
DQ404777_f
Nitrospinaceae
GU208445_f
AY771942_f
Planctomycetaceae
AM745150_f
FJ455877_f
GU455152_f
FJ517056_f
EU374107_f
EU374093_f
Clostridiaceae
Peptostreptococcaceae
Ruminococcaceae
JF344531_f
Thermoanaerobaculum_f
Thermodesulfovibrio_f
Nitrospiraceae
JF747669_f
DQ395502_f
DQ396300_f
Microthrix_f
AM991247_f
Phycisphaeraceae
HQ697838_f
HM066343_f
Caldilineaceae
DQ394964_f
DQ394955_f
EU385730_f
Z95718_f
EU374070_f
GU568020_f
AB021325_f
Prochlorococcaceae
GU553783_f
EU385821_f
AM997925_f
AB530233_f
OP8_f
GQ396871_f
AB240334_f
Gaiellaceae
EU700145_f
HM445331_f
EU686603_f
Ignavibacteriaceae
Saprospiraceae
AF407728_f
AB630582_f
GU145499_f
EU881211_f
EU795203_f
AF323761_f
EF574345_f
Sulfurovum_f
ETC

Fig. 4

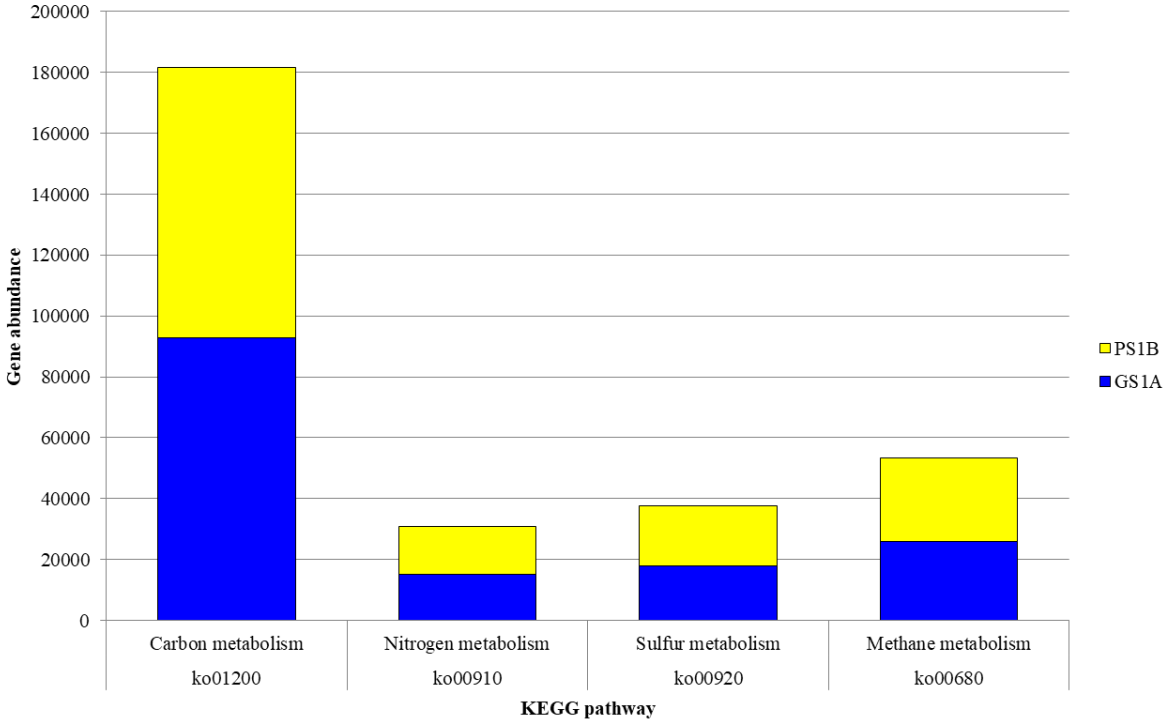

Fig. 5

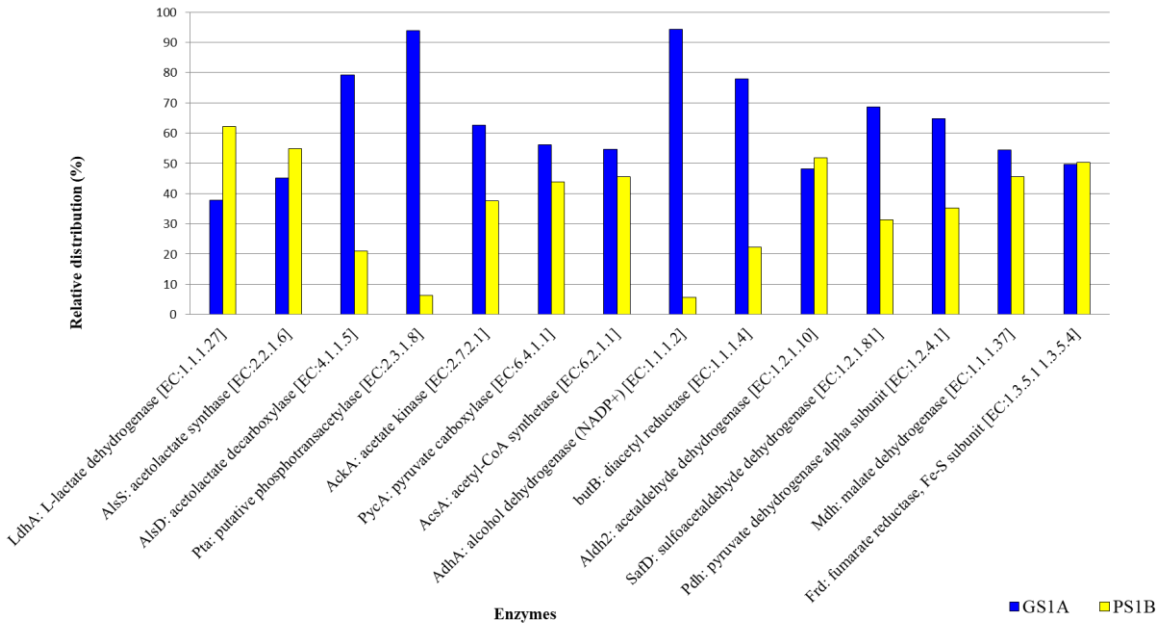

Fig. 6

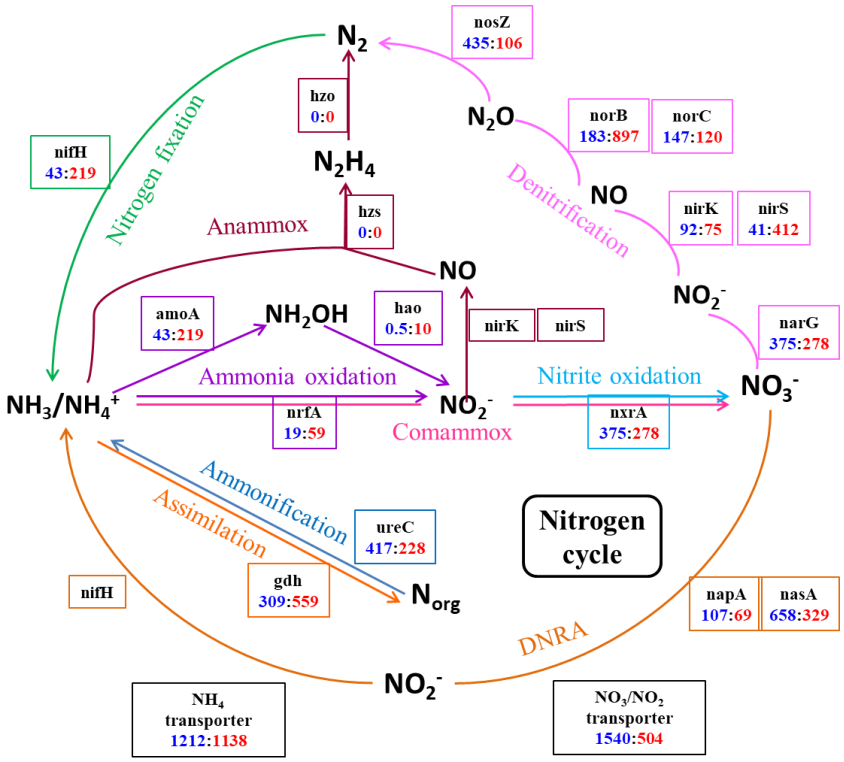
N2
nosZ
435:106
hzo
0:0
N2O
norB
183:897
norC
147:120
nifH
43:219
Nitrogen fixation
N2H4
Denitrification
NO
nirK
92:75
nirS
41:412
hzs
0:0
Anammox
NO
NO2-
amoA
43:219
NH2OH
hao
0.5:10
nirK
nirS
narG
375:278
Ammonia oxidation
Nitrite oxidation
NH3/NH4+
nrfA
19:59
NO2-
NO3-
Comammox
nxrA
375:278
Ammonification
Assimilation
ureC
417:228
Nitrogen cycle
gdh
309:559
Norg
nifH
napA
107:69
nasA
658:329
DNRA
NO2-
NH4 transporter
1212:1138
NO3/NO2 transporter
1540:504

Fig. 7

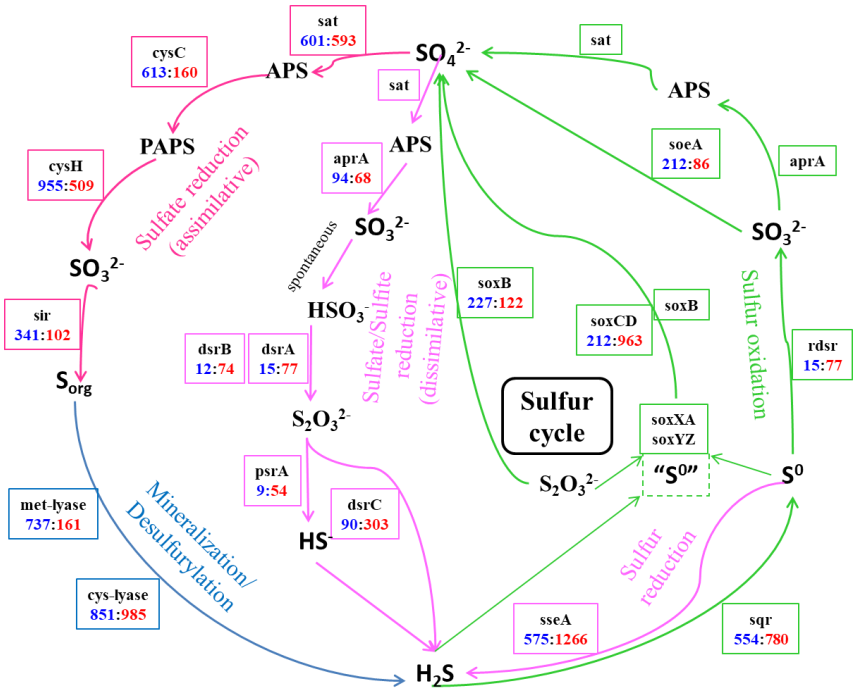
sat
601:593
cysC
613:160
SO4 2-
sat
APS
sat
APS
PAPS
APS
soeA
212:86
aprA
cysH
955:509
Sulfate reduction (assimilative)
aprA
94:68
SO3 2-
SO3 2-
spontaneous
SO3 2-
soxB
227:122
soxB
sir
341:102
HSO3-
soxCD
212:963
Sulfur oxidation
rdsr
15:77
dsrB
12:74
dsrA
15:77
Sulfate/Sulfite reduction (dissimilative)
Sorg
Sulfur cycle
S2O3 2-
soxXA
soxYZ
psrA
9:54
"S0"
S0
S2O3 2-
dsrC
90:303
HS-
met-lyase
737:161
Mineralization/ Desulfurylation
Sulfur reduction
cys-lyase
851:985
sseA
575:1266
sqr
554:780
H2S

Fig. 8

519 **REFERENCES:**

520 Arango, C. P., Tank, J. L., Schaller, J. L., Royer, T. V., Bernot, M. J., and David, M. B.: Benthic organic carbon
521 influences denitrification in streams with high nitrate concentration, Freshw. Biol., 52, 1210-1222,
522 doi:10.1111/j.1365-2427.2007.01758.x, 2007.

523 Azam, F., and Sajjad, M.: Colorimetric determination of organic carbon in soil by dichromate digestion in a
524 microwave oven, Pak. J. Biol. Sci, 8, 596-598, doi:10.3923/pjbs.2005.596.598, 2005.

525 Bernard, B. B., Bernard, H., and Brooks, J. M.: Determination of total carbon, total organic carbon and
526 inorganic carbon in sediments. In: TDI-Brooks International/B&B Labratories Inc. College Station, Texas,
527 1995.

528 Bertics, V. J., Löscher, C. R., Salonen, I., Dale, A. W., Gier, J., Schmitz, R. A., and Treude, T.: Occurrence of
529 benthic microbial nitrogen fixation coupled to sulfate reduction in the seasonally hypoxic Eckernförde Bay,
530 Baltic Sea, Biogeosciences, 10, 1243-1258, doi:10.5194/bg-10-1243-2013, 2013.

531 Bhushan, R., Dutta, K., and Somayajulu, B.: Concentrations and burial fluxes of organic and inorganic carbon
532 on the eastern margins of the Arabian Sea, Mar. Geol., 178, 95-113, doi:10.1016/S0025-3227(01)00179-7,
533 2001.

534 Bohlen, L., Dale, A. W., Sommer, S., Mosch, T., Hensen, C., Noffke, A., Scholz, F., and Wallmann, K.: Benthic
535 nitrogen cycling traversing the Peruvian oxygen minimum zone, Geochim. Cosmochim. Acta., 75, 6094-6111,
536 doi:10.1016/j.gca.2011.08.010, 2011.

537 Bristow, L. A., Callbeck, C. M., Larsen, M., Altabet, M. A., Dekaezemacker, J., Forth, M., Gauns, M., Glud, R.
538 N., Kuypers, M. M., and Lavik, G.: N_2 production rates limited by nitrite availability in the Bay of Bengal
539 oxygen minimum zone, Nat. Geosci., 10, 24-29, doi:10.1002/lom3.10126, 2017.

540 Callbeck, C. M., Lavik, G., Ferdelman, T. G., Fuchs, B., Gruber-Vodicka, H. R., Hach, P. F., Littmann, S.,
541 Schoffelen, N. J., Kalvelage, T., and Thomsen, S.: Oxygen minimum zone cryptic sulfur cycling sustained by
542 offshore transport of key sulfur oxidizing bacteria, Nat. Commun., 9, 1729-1740, doi:10.1038/s41467-018-
543 04041-x., 2018.

544 Canfield, D. E., Stewart, F. J., Thamdrup, B., De Brabandere, L., Dalsgaard, T., Delong, E. F., Revsbech, N. P.,
545 and Ulloa, O.: A cryptic sulfur cycle in oxygen-minimum–zone waters off the Chilean coast, Science, 330,
546 1375-1378, doi:10.1126/science.1196889, 2010.

547 Caporaso, J. G., Kuczynski, J., Stombaugh, J., Bittinger, K., Bushman, F. D., Costello, E. K., Fierer, N., Peña,
548 A. G., Goodrich, J. K., and Gordon, J. I.: QIIME allows analysis of high-throughput community sequencing
549 data, Nat. Methods, 7, 335-336, doi:10.1038/nmeth.f.303, 2010.

550 Choi, H., Koh, H.-W., Kim, H., Chae, J.-C., and Park, S.-J.: Microbial community composition in the marine
551 sediments of Jeju Island: next-generation sequencing surveys, J Microbiol Biotechnol, 26, 883-890,
552 doi:10.4014/jmb.1512.12036, 2016.

553 Chun, J., Lee, J.-H., Jung, Y., Kim, M., Kim, S., Kim, B. K., and Lim, Y.-W.: EzTaxon: a web-based tool for
554 the identification of prokaryotes based on 16S ribosomal RNA gene sequences, Int. J. Syst. Evol. Microbiol., 57,
555 2259-2261, doi:10.1099/ijs.0.64915-0, 2007.

556 Claesson, M. J., Wang, Q., O'Sullivan, O., Greene-Diniz, R., Cole, J. R., Ross, R. P., and O'Toole, P. W.:
557 Comparison of two next-generation sequencing technologies for resolving highly complex microbiota
558 composition using tandem variable 16S rRNA gene regions, Nucleic Acids Res., 38, e200,
559 doi:10.1093/nar/gkq873, 2010.

560 Cowie, G., Mowbray, S., Kurian, S., Sarkar, A., White, C., Anderson, A., Vergnaud, B., Johnstone, G., Brear,
561 S., and Woulds, C.: Comparative organic geochemistry of Indian margin (Arabian Sea) sediments: estuary to
562 continental slope, Biogeosciences, 11, 6683-6696, doi:10.5194/bg-11-6683-2014, 2014.

563 Dale, A. W., Sommer, S., Bohlen, L., Treude, T., Bertics, V. J., Bange, H. W., Pfannkuche, O., Schorp, T.,
564 Mattsdotter, M., and Wallmann, K.: Rates and regulation of nitrogen cycling in seasonally hypoxic sediments
565 during winter (Boknis Eck, SW Baltic Sea): Sensitivity to environmental variables, Estuar. Coast. Shelf Sci, 95,
566 14-28, doi:10.1016/j.ecss.2011.05.016, 2011.

567 Dang, H., Zhang, X., Sun, J., Li, T., Zhang, Z., and Yang, G.: Diversity and spatial distribution of sediment
568 ammonia-oxidizing crenarchaeota in response to estuarine and environmental gradients in the Changjiang
569 Estuary and East China Sea, Microbiology, 154, 2084-2095, doi:10.1099/mic.0.2007/013581-0, 2008.

de Voogd, N. J., Cleary, D. F., Polónia, A. R., and Gomes, N. C.: Bacterial community composition and predicted functional ecology of sponges, sediment and seawater from the thousand islands reef complex, West Java, Indonesia, FEMS Microbiol. Ecol., 91, fiv019, doi:10.1093/femsec/fiv019, 2015.

Devol, A. H.: Denitrification, anammox, and N_2 production in marine sediments, Annu. Rev. Mar. Sci., 7, 403-423, doi:10.1146/annurev-marine-010213-135040, 2015.

Diaz, R. J., and Rosenberg, R.: Spreading dead zones and consequences for marine ecosystems, Science, 321, 926-929, doi:10.1126/science.1156401, 2008.

Divya, B., Parvathi, A., Bharathi, P. L., and Nair, S.: 16S rRNA-based bacterial diversity in the organic-rich sediments underlying oxygen-deficient waters of the eastern Arabian Sea, World J. Microbiol. Biotechnol., 27, 2821-2833, doi:10.1007/s11274-011-0760-0, 2011.

Dyksma, S., Lenk, S., Sawicka, J. E., and Mußmann, M.: Uncultured Gammaproteobacteria and Desulfobacteraceae Account for Major Acetate Assimilation in a Coastal Marine Sediment, Front. Microbiol., 9, 3124-3124, doi:10.3389/fmicb.2018.03124, 2018.

Edgar, R. C.: Search and clustering orders of magnitude faster than BLAST, Bioinformatics, 26, 2460-2461, doi:10.1093/bioinformatics/btq461, 2010.

Eschbach, M., Schreiber, K., Trunk, K., Buer, J., Jahn, D., and Schobert, M.: Long-term anaerobic survival of the opportunistic pathogen *Pseudomonas aeruginosa* via pyruvate fermentation, J. Bacteriol, 186, 4596-4604, doi:10.1128/JB.186.14.4596-4604.2004, 2004.

Fernandes, G. L., Shenoy, B. D., Menezes, L. D., Meena, R. M., and Damare, S. R.: Prokaryotic Diversity in Oxygen Depleted Waters of the Bay of Bengal Inferred Using Culture-Dependent and-Independent Methods, Indian J. Microbiol., 59, 193-199, doi:10.1007/s12088-019-00786-1, 2019.

Fernandes, S., Mazumdar, A., Bhattacharya, S., Peketi, A., Mapder, T., Roy, R., Carvalho, M. A., Roy, C., Mahalakshmi, P., and Da Silva, R.: Enhanced carbon-sulfur cycling in the sediments of Arabian Sea oxygen minimum zone center, Sci. Rep., 8, 8665-8680, doi:10.1038/s41598-018-27002-2, 2018.

Fierer, N., and Jackson, R. B.: The diversity and biogeography of soil bacterial communities, Proc. Natl. Acad. Sci. U. S. A., 103, 626-631, doi:10.1016/j.apsoil.2019.06.008, 2006.

Froelich, P. N., Klinkhammer, G., Bender, M. a. a., Luedtke, N., Heath, G. R., Cullen, D., Dauphin, P., Hammond, D., Hartman, B., and Maynard, V.: Early oxidation of organic matter in pelagic sediments of the eastern equatorial Atlantic: suboxic diagenesis, Geochim. Cosmochim. Acta, 43, 1075-1090, doi:10.1016/0016-7037(79)90095-4, 1979.

Fuchs, B. M., Woebken, D., Zubkov, M. V., Burkill, P., and Amann, R.: Molecular identification of picoplankton populations in contrasting waters of the Arabian Sea, Aquat. Microb. Ecol., 39, 145-157, doi:10.3354/ame039145, 2005.

Fulweiler, R. W., Nixon, S. W., Buckley, B. A., and Granger, S. L.: Reversal of the net dinitrogen gas flux in coastal marine sediments, Nature, 448, 180-182, doi:10.1038/nature05963, 2007.

Ganesh, S., Parris, D. J., DeLong, E. F., and Stewart, F. J.: Metagenomic analysis of size-fractionated picoplankton in a marine oxygen minimum zone, ISME J., 8, 187-211, doi:10.1038/ismej.2013.144, 2014.

Gerdes, G., Klenke, T., and Noffke, N.: Microbial signatures in peritidal siliciclastic sediments: a catalogue, Sedimentology, 47, 279-308, doi:10.1046/j.1365-3091.2000.00284.x, 2000.

Gier, J., Sommer, S., Löscher, C. R., Dale, A. W., Schmitz, R. A., and Treude, T.: Nitrogen fixation in sediments along a depth transect through the Peruvian oxygen minimum zone, Biogeosciences, 13, 4065-4080, doi:10.5194/bg-13-4065-2016, 2016.

Gier, J., Löscher, C. R., Dale, A. W., Sommer, S., Lomnitz, U., and Treude, T.: Benthic Dinitrogen Fixation Traversing the Oxygen Minimum Zone Off Mauritania (NW Africa), Front. Mar. Sci., 4, doi:10.3389/fmars.2017.00390, 2017.

Glöckner, F. O., Fuchs, B. M., and Amann, R.: Bacterioplankton compositions of lakes and oceans: a first comparison based on fluorescence in situ hybridization, Environ Microbiol., 65, 3721–3726, doi:10.1128/aem.65.8.3721-3726., 1999.

Heaton, L., Fullen, M. A., and Bhattacharyya, R.: Critical analysis of the van Bemmelen conversion factor used to convert soil organic matter data to soil organic carbon data: Comparative analyses in a UK loamy sand soil, Espaço Aberto, 6, 35-44, doi:10.36403/espacoaberto.2016.5244, 2016.

Hodkinson, B. P., and Grice, E. A.: Next-generation sequencing: a review of technologies and tools for wound microbiome research, Adv. Wound Care, 4, 50-58, doi:10.1089/wound.2014.0542, 2015.

Horn, M. A., Ihssen, J., Matthies, C., Schramm, A., Acker, G., and Drake, H. L.: *Dechloromonas denitrificans* sp. nov., *Flavobacterium denitrificans* sp. nov., *Paenibacillus anaericanus* sp. nov. and *Paenibacillus terrae* strain MH72, N_2O-producing bacteria isolated from the gut of the earthworm *Aporrectodea caliginosa*, Int. J. Syst. Evol. Microbiol., 55, 1255-1265, doi:10.1099/ijs.0.63484-0, 2005.

Im, W.-T., Hu, Z.-Y., Kim, K.-H., Rhee, S.-K., Meng, H., Lee, S.-T., and Quan, Z.-X.: Description of *Fimbriimonas ginsengisoli* gen. nov., sp. nov. within the Fimbriimonadia class nov., of the phylum Armatimonadetes, Antonie van Leeuwenhoek, 102, 307-317, doi:10.1007/s10482-012-9739-6, 2012.

Iwai, S., Weinmaier, T., Schmidt, B. L., Albertson, D. G., Poloso, N. J., Dabbagh, K., and DeSantis, T. Z.: Piphillin: improved prediction of metagenomic content by direct inference from human microbiomes, PloS one, 11, e0166104, doi:10.1371/journal.pone.0166104., 2016.

Janssen, P. H.: Identifying the dominant soil bacterial taxa in libraries of 16S rRNA and 16S rRNA genes, Appl. Environ. Microbiol., 72, 1719-1728, doi:10.1128/AEM.72.3.1719-1728.2006, 2006.

Jensen, M. M., Lam, P., Revsbech, N. P., Nagel, B., Gaye, B., Jetten, M. S., and Kuypers, M. M.: Intensive nitrogen loss over the Omani Shelf due to anammox coupled with dissimilatory nitrite reduction to ammonium, ISME J., 5, 1660-1670, doi:10.1038/ismej.2011.44, 2011.

Krause, S., Liebetrau, V., Löscher, C. R., Böhm, F., Gorb, S., Eisenhauer, A., and Treude, T.: Marine ammonification and carbonic anhydrase activity induce rapid calcium carbonate precipitation, Geochim. Cosmochim. Acta, 243, 116-132, doi:10.1016/j.gca.2018.09.018, 2018.

Kümmel, S., Herbst, F.-A., Bahr, A., Duarte, M., Pieper, D. H., Jehmlich, N., Seifert, J., von Bergen, M., Bombach, P., Richnow, H. H., and Vogt, C.: Anaerobic naphthalene degradation by sulfate-reducing Desulfobacteraceae from various anoxic aquifers, FEMS Microbiol. Ecol., 91, 13, doi:10.1093/femsec/fiv006, 2015.

Langille, M. G., Zaneveld, J., Caporaso, J. G., McDonald, D., Knights, D., Reyes, J. A., Clemente, J. C., Burkepile, D. E., Thurber, R. L. V., and Knight, R.: Predictive functional profiling of microbial communities using 16S rRNA marker gene sequences, Nat. Biotechnol., 31, 814-821, doi:10.1038/nbt.2676, 2013.

Leloup, J., Loy, A., Knab, N. J., Borowski, C., Wagner, M., and Jørgensen, B. B.: Diversity and abundance of sulfate-reducing microorganisms in the sulfate and methane zones of a marine sediment, Black Sea, Environ. Microbiol., 9, 131-142, doi:10.1111/j.1462-2920.2006.01122.x, 2007.

Liu, J., Sun, F., Wang, L., Ju, X., Wu, W., and Chen, Y.: Molecular characterization of a microbial consortium involved in methane oxidation coupled to denitrification under micro-aerobic conditions, Microb. Biotechnol., 7, 64-76, doi:10.1111/1751-7915.12097, 2014.

Löscher, C. R., Mohr, W., Bange, H. W., and Canfield, D. E.: No nitrogen fixation in the Bay of Bengal?, Biogeosciences, 17, 851-864, doi:10.5194/bg-17-851-2020, 2020.

Luo, H., and Moran, M. A.: How do divergent ecological strategies emerge among marine bacterioplankton lineages?, Trends Microbiol., 23, 577-584, doi:10.1016/j.tim.2015.05.004, 2015.

Lv, X., Yu, J., Fu, Y., Ma, B., Qu, F., Ning, K., and Wu, H.: A meta-analysis of the bacterial and archaeal diversity observed in wetland soils, Sci. World J., 2014, 1-12, doi:10.1155/2014/437684, 2014.

Madigan, M., Cox, S. S., and Stegeman, R. A.: Nitrogen fixation and nitrogenase activities in members of the family Rhodospirillaceae, J. Bacteriol., 157, 73-78, doi:10.1128/JB.157.1.73-78.1984, 1984.

Maltby, J., Sommer, S., Dale, A. W., and Treude, T.: Microbial methanogenesis in the sulfate-reducing zone of surface sediments traversing the Peruvian margin, Biogeosciences, 13, 283-299, doi:10.5194/bg-13-283-2016, 2016.

Manske, A. K., Glaeser, J., Kuypers, M. M., and Overmann, J.: Physiology and phylogeny of green sulfur bacteria forming a monospecific phototrophic assemblage at a depth of 100 meters in the Black Sea, Appl. Environ. Microbiol., 71, 8049-8060, doi:10.1128/AEM.71.12.8049-8060.2005, 2005.

McCreary Jr, J. P., Yu, Z., Hood, R. R., Vinaychandran, P., Furue, R., Ishida, A., and Richards, K. J.: Dynamics of the Indian-Ocean oxygen minimum zones, Prog. Oceanogr., 112, 15-37, doi:10.1016/j.pocean.2013.03.002, 2013.

671 Mußmann, M., Pjevac, P., Krüger, K., and Dyksma, S.: Genomic repertoire of the Woeseiaceae/JTB255,
672 cosmopolitan and abundant core members of microbial communities in marine sediments, ISME J., 11, 1276-
673 1281, doi:10.1038/ismej.2016.185, 2017.

674 Naqvi, S., Naik, H., Pratihary, A., D'Souza, W., Narvekar, P., Jayakumar, D., Devol, A., Yoshinari, T., and
675 Saino, T.: Coastal versus open-ocean denitrification in the Arabian Sea, Biogeosciences, 3, 621-633,
676 doi:10.5194/bg-3-621-2006, 2006.

677 Naqvi, S. W. A., Lam, P., Narvenkar, G., Sarkar, A., Naik, H., Pratihary, A., Shenoy, D. M., Gauns, M., Kurian,
678 S., and Damare, S.: Methane stimulates massive nitrogen loss from freshwater reservoirs in India, Nat.
679 Commun., 9, 1265-1274, doi:10.1038/s41467-018-03607-z, 2018.

680 Narayan, N. R., Weinmaier, T., Laserna-Mendieta, E. J., Claesson, M. J., Shanahan, F., Dabbagh, K., Iwai, S.,
681 and DeSantis, T. Z.: Piphillin predicts metagenomic composition and dynamics from DADA2-corrected 16S
682 rDNA sequences, BMC genomics, 21, 1-12, doi:10.1186/s12864-020-6537-9, 2020.

683 Nelson, D., and Sommers, L.: Methods of soil analysis Part 2. Chemical and Microbiological Properties, in:
684 Total Carbon, Organic Carbon, and Organic Matter, American Society of Agronomy, Soil Science Society of
685 America, USA, 539-579, 1982.

686 Orsi, W. D., Coolen, M. J. L., Wuchter, C., He, L., More, K. D., Irigoien, X., Chust, G., Johnson, C.,
687 Hemingway, J. D., Lee, M., Galy, V., and Giosan, L.: Climate oscillations reflected within the microbiome of
688 Arabian Sea sediments, Sci. Rep., 7, 6040, doi:10.1038/s41598-017-05590-9, 2017.

689 Padilla, C. C., Bristow, L. A., Sarode, N., Garcia-Robledo, E., Ramírez, E. G., Benson, C. R., Bourbonnais, A.,
690 Altabet, M. A., Girguis, P. R., and Thamdrup, B.: NC10 bacteria in marine oxygen minimum zones, ISME J.,
691 10, 2067, doi:10.1038/ismej.2015.262, 2016.

692 Pattan, J., Mir, I. A., Parthiban, G., Karapurkar, S. G., Matta, V., Naidu, P., and Naqvi, S.: Coupling between
693 suboxic condition in sediments of the western Bay of Bengal and southwest monsoon intensification: A
694 geochemical study, Chem. Geol., 343, 55-66, doi:10.1016/j.chemgeo.2013.02.011, 2013.

695 Paulmier, A. D. R.-P.: Oxygen minimum zones (OMZs) in the modern ocean, Prog. Oceanogr., 80, 113–128,
696 doi:10.1016/j.pocean.2008.08.001, 2009.

697 Penton, C. R., Devol, A. H., and Tiedje, J. M.: Molecular evidence for the broad distribution of anaerobic
698 ammonium-oxidizing bacteria in freshwater and marine sediments, Appl. Environ. Microbiol., 72, 6829-6832,
699 doi:10.1128/AEM.01254-06., 2006.

700 Pitcher, A., Villanueva, L., Hopmans, E. C., Schouten, S., Reichart, G.-J., and Damsté, J. S. S.: Niche
701 segregation of ammonia-oxidizing archaea and anammox bacteria in the Arabian Sea oxygen minimum zone,
702 ISME J., 5, 1896, doi:10.1038/ismej.2011.60, 2011.

703 Pramanik, A., Basak, P., Banerjee, S., Sengupta, S., Chattopadhyay, D., and Bhattacharyya, M.: Metagenomic
704 exploration of the bacterial community structure at Paradip Port, Odisha, India, Genom. Data, 7, 94-96,
705 doi:10.1016/j.gdata.2015.12.005, 2016.

706 Quast, C., Pruesse, E., Yilmaz, P., Gerken, J., Schweer, T., Yarza, P., Peplies, J., and Glöckner, F. O.: The
707 SILVA ribosomal RNA gene database project: improved data processing and web-based tools, Nucleic Acids
708 Res., 41, D590-D596, doi:10.1093/nar/gks1219, 2012.

709 Quince, C., Lanzen, A., Davenport, R. J., and Turnbaugh, P. J.: Removing noise from pyrosequenced amplicons,
710 BMC Bioinf., 12, 38, doi:10.1186/1471-2105-12-38, 2011.

711 Rajpathak, S. N., Banerjee, R., Mishra, P. G., Khedkar, A. M., Patil, Y. M., Joshi, S. R., and Deobagkar, D. D.:
712 An exploration of microbial and associated functional diversity in the OMZ and non-OMZ areas in the Bay of
713 Bengal, J. Biosci., 43, 635-648, doi:10.1007/s12038-018-9781-2, 2018.

714 Ramaswamy, V., and Gaye, B.: Regional variations in the fluxes of foraminifera carbonate, coccolithophorid
715 carbonate and biogenic opal in the northern Indian Ocean, Deep Sea Res. Part I, 53, 271-293,
716 doi:10.1016/j.dsr.2005.11.003, 2006.

717 Ramos, H. C., Hoffmann, T., Marino, M., Nedjari, H., Presecan-Siedel, E., Dreesen, O., Glaser, P., and Jahn, D.:
718 Fermentative metabolism of *Bacillus subtilis*: physiology and regulation of gene expression, J. Bacteriol, 182,
719 3072-3080, doi:10.1128/JB.182.11.3072-3080.2000, 2000.

Robinson, R. S., Kienast, M., Luiza Albuquerque, A., Altabet, M., Contreras, S., De Pol Holz, R., Dubois, N., Francois, R., Galbraith, E., and Hsu, T. C.: A review of nitrogen isotopic alteration in marine sediments, Paleoceanogr., 27, doi:10.1029/2012PA002321, 2012.

Sarma, V., Kumar, M. D., and Saino, T.: Impact of sinking carbon flux on accumulation of deep-ocean carbon in the Northern Indian Ocean, Biogeochemistry, 82, 89-100, doi:10.1007/s10533-006-9055-1, 2007.

Sarma, V., Krishna, M., Viswanadham, R., Rao, G., Rao, V., Sridevi, B., Kumar, B., Prasad, V., Subbaiah, C. V., and Acharyya, T.: Intensified oxygen minimum zone on the western shelf of Bay of Bengal during summer monsoon: influence of river discharge, J. Oceanogr., 69, 45-55, doi:10.1007/s10872-012-0156-2, 2013.

Schimel, J. P., and Schaeffer, S. M.: Microbial control over carbon cycling in soil, Front. Microbiol., 3, 348-358, doi:10.3389/fmicb.2012.00348, 2015.

Schloss, P. D., Westcott, S. L., Ryabin, T., Hall, J. R., Hartmann, M., Hollister, E. B., Lesniewski, R. A., Oakley, B. B., Parks, D. H., and Robinson, C. J.: Introducing mothur: open-source, platform-independent, community-supported software for describing and comparing microbial communities, Appl. Environ. Microbiol., 75, 7537-7541, doi:10.1128/AEM.01541-09, 2009.

Schunck, H., Lavik, G., Desai, D. K., Großkopf, T., Kalvelage, T., Löscher, C. R., Paulmier, A., Contreras, S., Siegel, H., and Holtappels, M.: Giant hydrogen sulfide plume in the oxygen minimum zone off Peru supports chemolithoautotrophy, PloS one, 8, e68661, doi:10.1371/journal.pone.0068661, 2013.

Shao, M.-F., Zhang, T., and Fang, H. H.-P.: Sulfur-driven autotrophic denitrification: diversity, biochemistry, and engineering applications, Appl. Microbiol. Biotechnol., 88, 1027-1042, doi:10.1007/s00253-010-2847-1, 2010.

Stewart, F. J., Ulloa, O., and DeLong, E. F.: Microbial metatranscriptomics in a permanent marine oxygen minimum zone, Environ. Microbiol., 14, 23-40, doi:10.1111/j.1462-2920.2010.02400.x, 2012.

Suh, S.-S., Park, M., Hwang, J., Lee, S., Moh, S. H., Park, K. H., and Lee, T.-K.: Characterization of bacterial communities associated with seasonal water masses from Tongyoung in South Sea of Korea, Ocean Sci. J., 49, 193-200, doi:10.1007/s12601-014-0019-4, 2014.

Ulloa, O., Wright, J. J., Belmar, L., and Hallam, S. J.: Pelagic oxygen minimum zone microbial communities, in: The Prokaryotes, edited by: Rosenberg E., DeLong E.F., Lory S., Stackebrandt E., and F., T., Springer, Berlin, Heidelberg, 113-122, 2013.

van der Weijden, C. H., Reichart, G. J., and Visser, H. J.: Enhanced preservation of organic matter in sediments deposited within the oxygen minimum zone in the northeastern Arabian Sea, Deep Sea Res. Part II, 46, 807-830, doi:10.1016/S0967-0637(98)00093-4, 1999.

Varki, A., and Gagneux, P.: Biological functions of glycans, in: Essentials of Glycobiology [Internet]. 3rd edition, Cold Spring Harbor Laboratory Press, 2017.

Wang, Y., Sheng, H.-F., He, Y., Wu, J.-Y., Jiang, Y.-X., Tam, N. F.-Y., and Zhou, H.-W.: Comparison of the levels of bacterial diversity in freshwater, intertidal wetland, and marine sediments by using millions of illumina tags, Appl. Environ. Microbiol., 78, 8264-8271, doi:10.1128/AEM.01821-12, 2012.

Ward, B., Devol, A., Rich, J., Chang, B., Bulow, S., Naik, H., Pratihary, A., and Jayakumar, A.: Denitrification as the dominant nitrogen loss process in the Arabian Sea, Nature, 461, 78-82, doi:10.1038/nature08276, 2009.

Wegner, C.-E., Richter-Heitmann, T., Klindworth, A., Klockow, C., Richter, M., Achstetter, T., Glöckner, F. O., and Harder, J.: Expression of sulfatases in *Rhodopirellula baltica* and the diversity of sulfatases in the genus *Rhodopirellula*, Mar. Genomics, 9, 51-61, doi:10.1016/j.margen.2012.12.001, 2013.

West, N. J., Schönhuber, W. A., Fuller, N. J., Amann, R. I., Rippka, R., Post, A. F., and Scanlan, D. J.: Closely related *Prochlorococcus* genotypes show remarkably different depth distributions in two oceanic regions as revealed by in situ hybridization using 16S rRNA-targeted oligonucleotides, Microbiology, 147, 1731-1744, doi:10.1099/00221287-147-7-1731, 2001.

Yakimov, M. M., Giuliano, L., Gentile, G., Crisafi, E., Chernikova, T. N., Abraham, W.-R., Lünsdorf, H., Timmis, K. N., and Golyshin, P. N.: *Oleispira antarctica* gen. nov., sp. nov., a novel hydrocarbonoclastic marine bacterium isolated from Antarctic coastal sea water, Int. J. Syst. Evol. Microbiol., 53, 779-785, doi:10.1099/ijs.0.02366-0, 2003.

Yanagibayashi, M., Nogi, Y., Li, L., and Kato, C.: Changes in the microbial community in Japan Trench sediment from a depth of 6292 m during cultivation without decompression, FEMS Microbiol. Lett., 170, 271-279, doi:10.1111/j.1574-6968.1999.tb13384.x, 1999.

Yu, Z., Wang, X., Han, G., Liu, X., and Zhang, E.: Organic and inorganic carbon and their stable isotopes in surface sediments of the Yellow River Estuary, Sci. Rep., 8, 1-10, doi:10.1038/s41598-018-29200-4, 2018.

Zhu, D., Tanabe, S.-H., Yang, C., Zhang, W., and Sun, J.: Bacterial community composition of South China Sea sediments through pyrosequencing-based analysis of 16S rRNA genes, PloS one, 8, e78501, doi:10.1371/journal.pone.0078501, 2013.